



Coastal Zone – Appendix

Collection 10

Version 1

General coordinator

Pedro Walfir Martins e Souza Filho

Team

Cesar Guerreiro Diniz

Júlia Ascencio Cansado

Luiz Cortinhas Ferreira Neto

Maria Luíze Silva Pinheiro

1 Overview

The Brazilian coastal zone presents diverse environments that evolved during the Quaternary in response to climate and sea-level changes. These environments show an interaction between different sediment supplies and a geologic heritage that dates back to the breakup of South America and Africa (Dominguez, 2009; Souza-Filho et al., 2023). Among this diversity of coastal features, five classes are mapped in the MapBiomass Collection 10: Mangroves, Beaches, Dunes and Sand Spots, Aquaculture, Hypersaline Tidal Flats, and Shallow Coral Reefs.

Table 1 shows the evolution of coastal features mapped in each collection and the changes in its methodological aspects.

Table 1 - Overview of the Coastal MapBiomass Collections since their first version. In the method column, 'EDT' means 'Empirical Decision Tree,' RF refers to 'Random Forest,' and U-Net refers to a CNN-based Deep-Learning method.

Collection	Range	Method	Classes	Improvements
1.0	2008-2015	EDT	No Coastal-Specific Mappings	- First collection
2.0	2000-2016	EDT	Mangroves, Beaches & Dunes	- First two coastal classes
2.3	1985-2016	EDT	Same as Collection 2.0	--
3.0	1985-2017	RF	Mangroves, Beaches & Dunes	- Random Forest - Temporal stability is used to generate a large training dataset - Expanded to the entire Landsat Temporal Series - Better Quality Median Composites
3.1	1985-2017	RF	Same as Collection 3.0	--
4.0	1985-2018	RF and U-net	Mangroves, Beaches, and Dunes, Aquaculture	- Aquaculture/Salt-culture is added as a coastal feature - Improvements in temporal consistency through additional post-processing/ filters
4.1	1985-2018	RF and U-net	Same as Collection 4.0	--
5.0	1985-2019	RF and U-net	Mangroves, Beaches & Dunes, Aquaculture, Hypersaline Tidal Flats	- Hypersaline Tidal Flats are added as a coastal feature (also known as "Apicum")
6.0	1985-2020	RF and U-net	Mangroves, Beaches, Dunes and Sand-Spots, Aquaculture, Hypersaline Tidal Flats	- Sand Spots is now a feature that integrates Beach and Dune, coastal class
7.0	1985-2021	RF and U-net	Same as Collection 6	- A new version of the U-net classifier.
7.1	1985-2021	RF and U-net	Same as Collection 7	--
8.0	1985-2022	RF and U-net	Same as Collection 7.1	- Enhancements of the Deep-Learning Algorithms - Enhancements in temporal consistency through additional post-processing/ filters
9.0	1985-2023	RF and U-net	Mangroves, Beaches, Dunes and Sand-Spots, Aquaculture, Hypersaline Tidal Flats and Shallow Coral Reefs	- Shallow Coral Reefs are added as a coastal feature

10.0	1985-2024	RF and U-net	Same as Collection 9	<ul style="list-style-type: none"> - Aquaculture is now being mapped throughout Brazil, not only in Coastal Zone - Resampling of Beach, Dune and Sand Spots
------	-----------	--------------	----------------------	---

Compared to Collection 8, Collection 9 of the coastal zone mapping presents a new class of coastal features, the Shallow Coral Reefs, here defined as “an underwater ecosystem characterized by reef-building corals, formed of colonies of coral polyps held together by calcium carbonate” (Ferreira and Maida, 2006). Most coral reefs are built from stony corals, whose polyps cluster in groups. However, small methodological changes were made. Two machine learning techniques were used: Mangrove, Beach, Dunes and Sand Spots, Shallow Coral Reefs based on Random Forests, and Aquaculture and Hypersaline Tidal Flat are U-net derived. In Collection 9, the “Apicum”/Hypersaline Tidal Flat theme gained its third generation of the U-Net learning model, which helped reduce its area oscillation and commission and omission errors.

In the newest Collection (10), Aquaculture has been mapped throughout the whole country, not only on the Coastal Zone, and Beaches, Dunes and Sand Spots has been resampled, aiming to fix some issues the class had with the limits used in the integration process in the previous collections, which cropped parts of it.

The classification/segmentation, validation, and publication workflow is described in Figure 1. The code repository can be accessed:

- Aquaculture: <https://github.com/mapbiomas/brazil-aquaculture>
- Coastal Zone: <https://github.com/mapbiomas/brazil-coastal-zone>

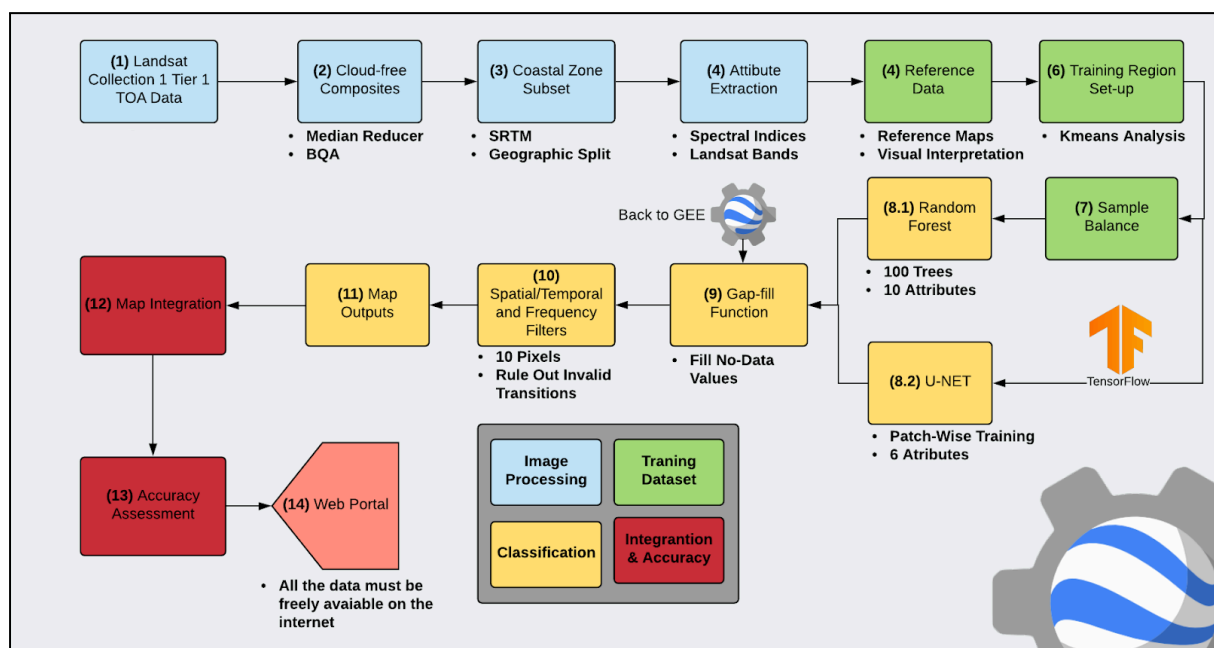


Figure 1 - Workflow of Coastal Zone mapping, validation, and publication. All data processing occurs within the Google Earth Engine - GEE platform, except for the aquaculture/saline pattern and hypersaline tidal flats segmentation, dependent on the

TensorFlow library. In green are steps related to sampling design. In yellow are steps related to classification. The mapping accuracy evaluation stage is in red. **(1)** Range from 1985 to 2024.

2 Landsat image mosaics

The cross-cutting theme “Coastal Zone” classification used Landsat mosaics that differed from those used to classify the natural vegetation of the Brazilian biomes. The coastal mosaics were defined to preserve the maximum of the coastal zone land area while capturing the minor possible cloud cover. These Landsat mosaics are the third generation of the methodology developed specifically for these cross-cutting themes.

2.1 Definition of the temporal period

Coastal areas are severely affected by atmospheric nebulosity, intensified by their proximity to the oceans and tropical locations. On the other hand, the attempt to identify a time interval that covers only the driest season of the year as an alternative to reduce cloud persistence severely reduces the number of images available to cover the entire coastal region. Thus, the annual cloud-free composites are generated, ranging from the 1st of January to the 31st of December.

2.2 Mosaic Subsets

Since the Brazilian coastal zone (BCZ) is an extensive region, approximately 8,500 kilometers from Oiapoque to Chui (not taking reentrances into account), and affected by various atmospheric systems with lesser or greater nebulosity influence, the BCZ is divided into seven different sectors (Figure 2).

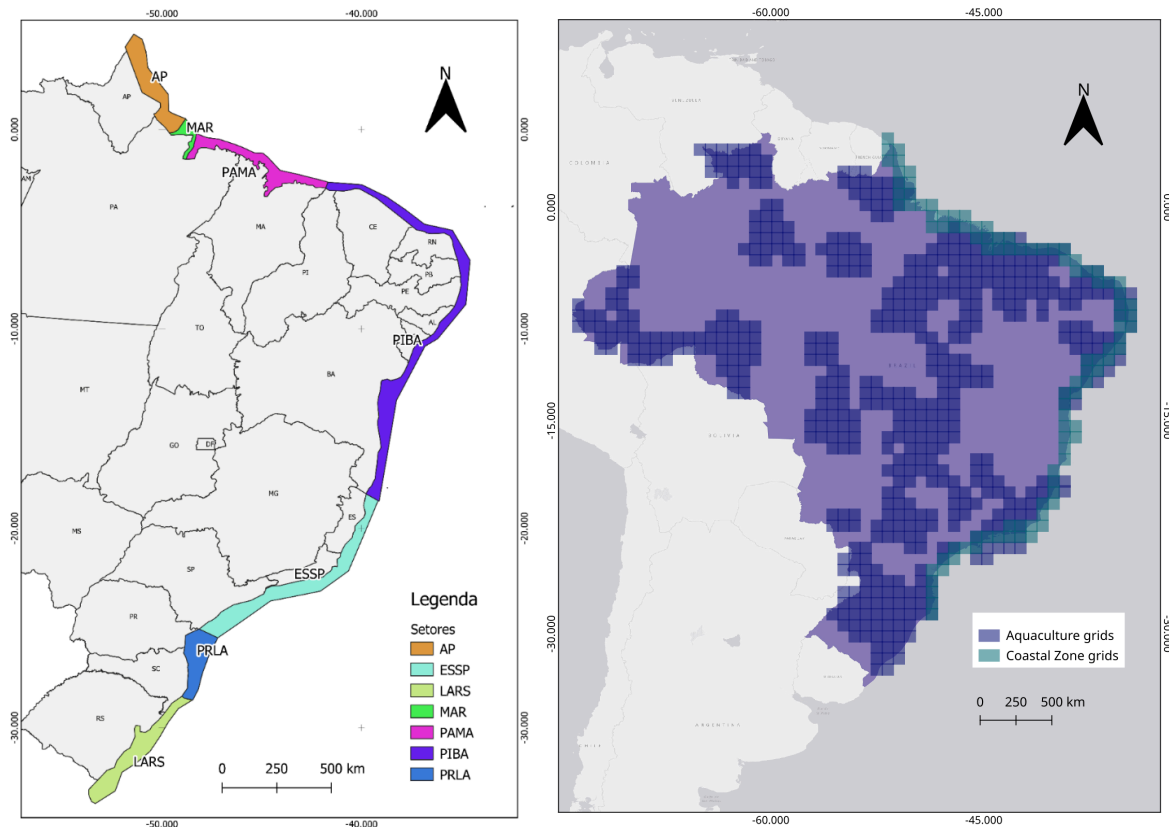


Figure 2 (LEFT) - The seven Brazilian Coastal Zone sectors used for mosaic subsets and image classification. Sector 1 - Amapá (AP), coastal region of Amapá. Sector 2 - Marajó Island (MAR), coastal region of Marajó Island. Sector 3 - Pará / Maranhão (PAMA), a coastal sector of the states of Pará and Maranhão. Piauí / Bahia (PIBA) is a coastal sector of the states of Piauí to Bahia. Sector 5 - Espírito Santo / São Paulo (ESSP), a region that includes the states of Espírito Santo and São Paulo. Sector 6 – Paraná/Laguna (PRLA), a coastal area that goes from the state of Paraná to the municipality of Laguna in Santa Catarina, and finally, Sector 7 (LARS), a region that ranges from Laguna to the state of Rio Grande do Sul. (RIGHT) - Search areas used for Aquaculture class, based on São José et al. (2022).

2.3 Image selection

Since the MapBiomass Collection 2.3, substituting the "Simple Cloud Score" method used in previous collections, the cloud/shadow removal script started to combine the Landsat QA band values and the GEE median reducer. In Landsat Collection 2 Tier 1 data, each pixel in the QA band contains unsigned integer values representing specific surface, atmospheric, and sensor conditions that may affect the overall usefulness of a given pixel. When effectively used, QA values can improve the data integrity by indicating which pixels might be affected by instrument artifacts or subject to cloud contamination (USGS, 2017). In conjunction, GEE can be instructed to pick the median pixel values in a stack of images. By doing so, GEE rejects values that are too high (e.g., clouds) or too low (e.g., shadows) and picks the median pixel value in each band over time. This operation has improved over several collections, and it is possible to see the difference between two "cloud-free composites" from different collections below (Figure 3).



Figure 3 - Left, MapBiomass Collection 2 “cloud-free composite.” Right, MapBiomass Collection 10 “cloud-free composite.”

2.4 Final quality

The mosaic quality is related to Landsat’s cloud-free availability during the image selection period. However, from 1985 to March 1998, only the Landsat 5 satellite remained operational. The BCZ’s average number of images per year was ~500 during this period. In the last decade, between 2015 and 2024, this figure quadruple to ~2200 images per year, as shown in Figure 4.

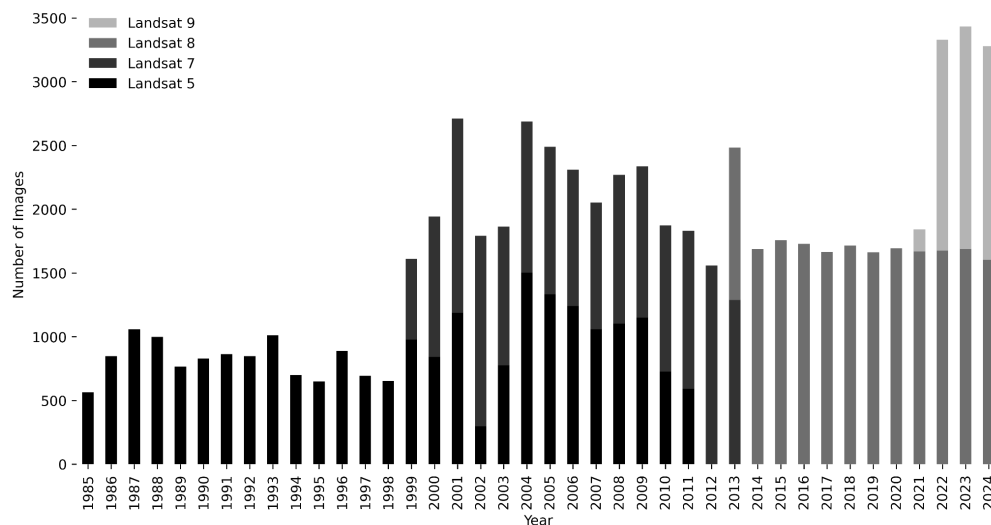


Figure 4 – Landsat image availability from 1985 to 2024. The bars show the distribution of Landsat images along the time series.

3 Detection

The automatic classification of the Landsat mosaics was mainly performed on the Google Earth Engine platform, based on the Random Forest classifier (Breiman, 2001). The Hypersaline Tidal Flat and the Aquaculture classes were deep-learning derived and thus segmented on local environment.

3.1 Detection scheme

Each class was mapped separately as a binary variable. Therefore, five independent detection processes were performed: 1) Mangrove, 2) Beaches and Dunes and Sand Spots, 3) Hypersaline Tidal Flats , 4) Aquaculture, and 5) Shallow Coral Reefs. The mapping process was carried out considering only two possible classes for each pixel: the interest class (Mangrove, Beaches, Dunes and Sand Spots, Hypersaline Tidal Flat (HTF), Aquaculture, and Shallow Coral Reef) or the non-interest class (all the non-classes of each target of interest).

We have selected training points based on the availability of reference maps and the previous MapBiomass Collection. The following sections present the details of the parameters used in the image classifiers, the reference maps used for each interest class, and the feature space produced for each classification.

3.2 Reference Data

A dataset of reference data was used to guide the generation of training samples for each class. Table 2 shows the references used for each of the coastal zone classes.

Table 2 - Reference datasets to guide training samples of coastal zone classes in Collection 9.

Class	References
Mangrove	MapBiomass Collection 8, Giri et al., 2011, ICMBio Mangrove Atlas (ICMBio, 2018), Global Mangrove Watch (Bunting <i>et al.</i> , 2018; Thomas <i>et al.</i> , 2018), Diniz et al., 2019, Panorama da Conservação dos Ecossistemas Costeiros e Marinhos no Brasil (MMA, 2010), plus visual inspection.
Aquaculture/Salt-Culture	MapBiomass Collection 8, Atlas Dos Remanescentes Florestais da Mata Atlântica (SOS Mata Atlântica, 2020), Barbier and Cox, 2003; Guimarães et al., 2010; Prates, Gonçalves and Rosa, 2010, Queiroz et al., 2013; Tenório et al., 2015; Thomas et al., 2017, Diniz et al., 2021, São José, F. F. de et al., 2022, plus visual inspection
Apicum/Hypersaline Tidal Flat	MapBiomass Collection 8, Atlas Dos Remanescentes Florestais da Mata Atlântica (SOS Mata Atlântica, 2020), Prates, Gonçalves and Rosa, 2010, Panorama da Conservação dos Ecossistemas Costeiros e Marinhos no Brasil (MMA, 2010), plus visual inspection.
Beaches, Dunes and Sand Spots	MapBiomass Collection 8, Atlas Dos Remanescentes Florestais da Mata Atlântica (SOS Mata Atlântica, 2020), Prates, Gonçalves and Rosa, 2010, Panorama da Conservação dos Ecossistemas Costeiros e Marinhos no Brasil (MMA, 2010), plus visual inspection.

Shallow Coral Reef	Áreas Prioritárias para Conservação da Biodiversidade (MMA), Panorama da Conservação dos Ecossistemas Costeiros e Marinhos no Brasil (MMA, 2010), Atlas dos Recifes de Corais nas Unidades de Conservação Brasileiras (MMA), Allen Coral Reef Atlas, and UNEP-WCMC Global Distribution of Coral Reefs.
--------------------	--

3.3 Coastal Zone Feature Space

Tables 3 and 4 show all spectral indices and bands used for the BCZ detection.

Table 3 – Spectral Indices used for coastal zone classification.

Index	Expression	Reducer	Reference
EVI2	$2.5 * ((\text{NIR} - \text{RED}) / (\text{NIR} + 2.4 * \text{RED} + 1))$	Median and Standard Deviation	Liu and Huete, 1995
NDVI	$(\text{NIR} - \text{RED}) / (\text{NIR} + \text{RED})$	Median and Standard Deviation	Tucker, 1979
MNDWI	$(\text{GREEN} - \text{SWIR1}) / (\text{GREEN} + \text{SWIR1})$	Median and Standard Deviation	Xu, 2006
NDSI	$(\text{SWIR1} - \text{NIR}) / (\text{SWIR1} + \text{NIR})$	Median and Standard Deviation	Rogers and Kearney, 2004
MMRI	Modular Mangrove Recognition Index	Median and Standard Deviation	Diniz et al., 2019
GBNDVI	The Green Blue NDVI	Median and Standard Deviation	Wang et al., 2007
GRNDVI	The Green Red NDVI	Median and Standard Deviation	Wang et al., 2007
GARI	Green Atmospherically Resistant Vegetation Index	Median and Standard Deviation	Gitelson et al., 2003
CI	Coloration Index	Median and Standard Deviation	Escadafal et al., 1994

Table 4 - Table of bands used to classify coastal zone classes.

Variable	Description	Reducer
GREEN	Landsat Green band median value	Median and Standard Deviation
RED	Landsat Red band median value	Median and Standard Deviation
NIR	Landsat NIR band median value	Median and Standard Deviation
SWIR1	Landsat SWIR1 band median value	Median and Standard Deviation

SWIR2	Landsat SWIR2 band median value	Median and Standard Deviation
-------	---------------------------------	-------------------------------

3.4 Detection strategy, training samples, and parameters

When reference maps that match the classes and/or year to be mapped, reference maps of the closest possible timeframe to the median composites were used. When no reference map was available, then the detection results of the previous year were used for subsequent training. Tables 5 and 6 show the Random Forest and U-net parameters used to detect each one of the years.

Table 5 - Random Forest parameters used to classify each one of the years. Mangroves, beaches, dunes, sand spots, and shallow coral reefs.

Parameter	Value
Number of trees	100
Samples	50000 (non-target), 5000 (target)
Classes	2 (binary classification)

Table 6—U-Net parameters used to segment each year. The U-Net-derived classes are the aquaculture and HTF classes.

Parameter	Value
Model	U-Net
Patch Size	256 x 256 px
Optimizer	Nadam
Learning Rate	5×10^{-6}
Samples	Aqua: 34600 (train), 14200 (validation) HTF: 47700 (train), 13355 (validation)
Attributes	Green, Red, Nir, Swir 1, NDVI, MNDWI
Output	binary segmentation

3.4.1 Mangroves

As with any supervised method, the Random Forest classifier must rely on a training dataset. For mangrove cover recognition, the training data was obtained from MapBiomass Collection 8, Giri et al., 2011, Atlas dos Manguezais do Brasil (ICMBio, 2018), Global Mangrove Watch (Bunting *et al.*, 2018; Thomas *et al.*, 2018) and visual inspection (Figure 5). The consolidated results of the mangrove distributions are available in Diniz et al., 2019.

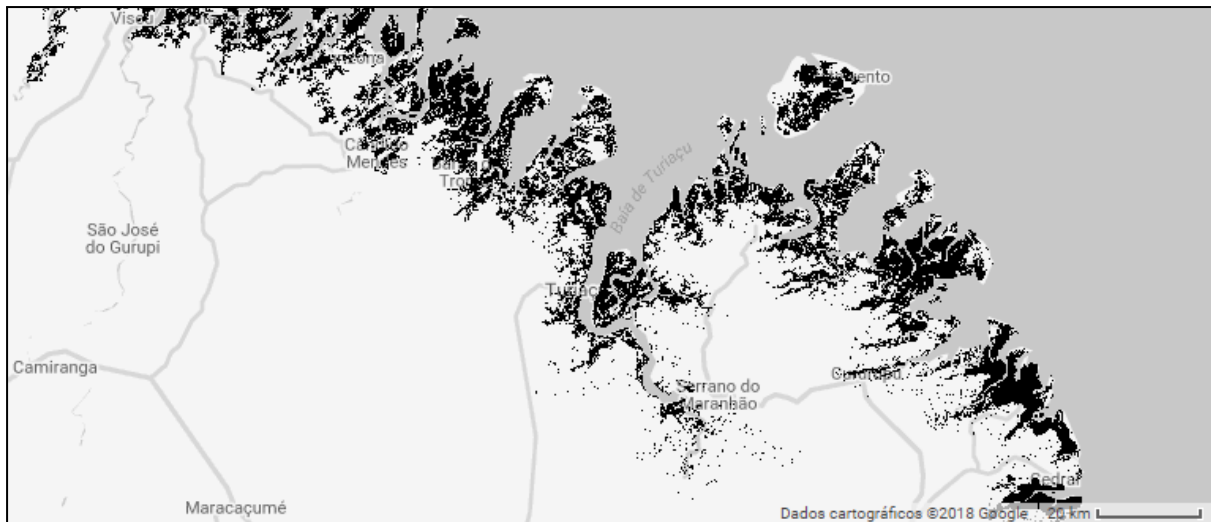


Figure 5 - Global Mangrove Cover data was used as a mangrove mapping reference from 1999 to 2002.

3.4.2 Hypersaline Tidal Flat

Generally, a mangrove swamp's less frequently flooded area, in the transition to topographically elevated lands, is usually devoid of arboreal vegetation. This area is called “Apicum” in Brazil. In the international scientific literature, this transition zone is usually called hypersaline tidal flat. As shown in Table 1, three different reference maps were here used: the “Atlas dos Remanescentes Florestais da Mata Atlântica” (SOS Mata Atlântica, 2020) from 2019/2020, covering the Mata Atlantica coastal region and the “Carta de Sensibilidade Ambiental ao Óleo - Pará-Maranhão-Barreirinhas” referent to 2017 and covering most of the Brazilian north coastal area and the data from the MapBiomass Collection 8 (Figure 6).



Figure 6 – Apicum reference maps, the “Atlas Dos Remanescentes Florestais da Mata Atlântica” from 2019/2020, covering the Forest Atlantic coastal region and the “Carta de Sensibilidade Ambiental ao Óleo -Pará-Maranhão-Barreirinhas 2017”, covering most of the Brazilian north coast region.

3.4.3 Beaches, Dunes and Sand Spots

Mapped in a single class, here “Beaches, Dunes and Sand Spots” refers to sandy strands, bright white, with no vegetation predominance. As shown in Table 1, the training data for this land cover was obtained from MapBiomias Collection 8 and other available reference data (Table 2; Figure 7).

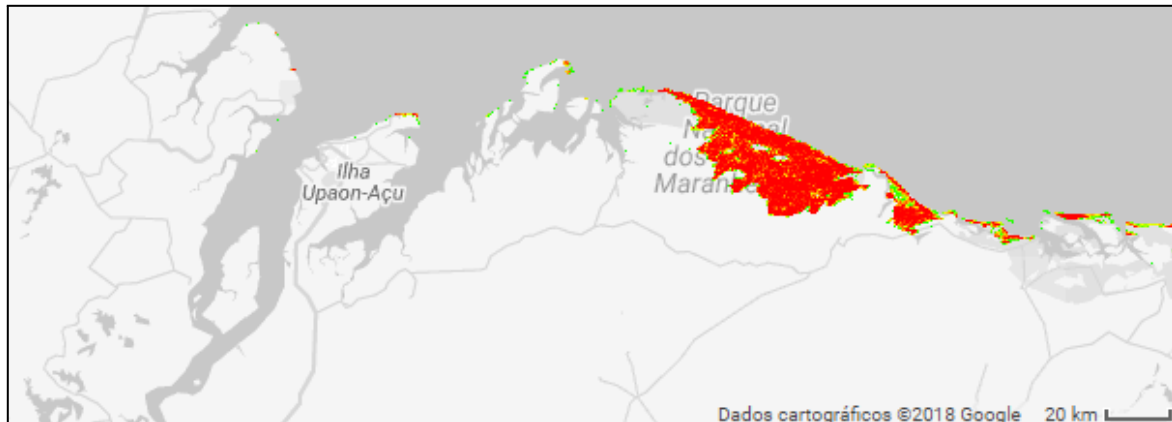


Figure 7 - The training data for this land cover was obtained from MapBiomias Collection 8 and available reference, as sThis”.

3.4.4 Aquaculture/Salt Culture

Compared to previous Mapbiomas Collections, Collection 10 aquaculture mapping consolidated the use of the Deep-Learning model in replacement of the traditional Random Forest Algorithm (Diniz *et al.*, 2021), and has detected aquaculture beyond BCZ. In this scenario, conventional machine learning algorithms use spectral-temporal data to classify targets according to similarities of their spectral-temporal patterns (Breiman, 2001). However, temporal and spectral properties might not be enough to discriminate “super-similar” targets (targets that behave similarly in both spectral and temporal domains). That is the case for most surface water targets, such as aquaculture ponds, rivers, lakes, and open waters (Figure 8).

Unless water presents a high concentration of external compounds (minerals, suspended sediments, algae, and others), not much can be done to spectrally differentiate between numerous surface water targets. On the other hand, the temporal domain may not present much valid discriminatory data either. In Brazil, aquaculture is a traditional and coastal-related economic activity. Thus, in 35 years of data, a diverse set of aquaculture frequencies may exist (Barbier and Cox, 2003; Guimarães *et al.*, 2010; Queiroz *et al.*, 2013; Tenório *et al.*, 2015; Thomas *et al.*, 2017). As a result, the temporal domain fails to distinguish between well-consolidated aquaculture, main river channels, and open waters once all these features present high temporal persistence throughout the entire time series.

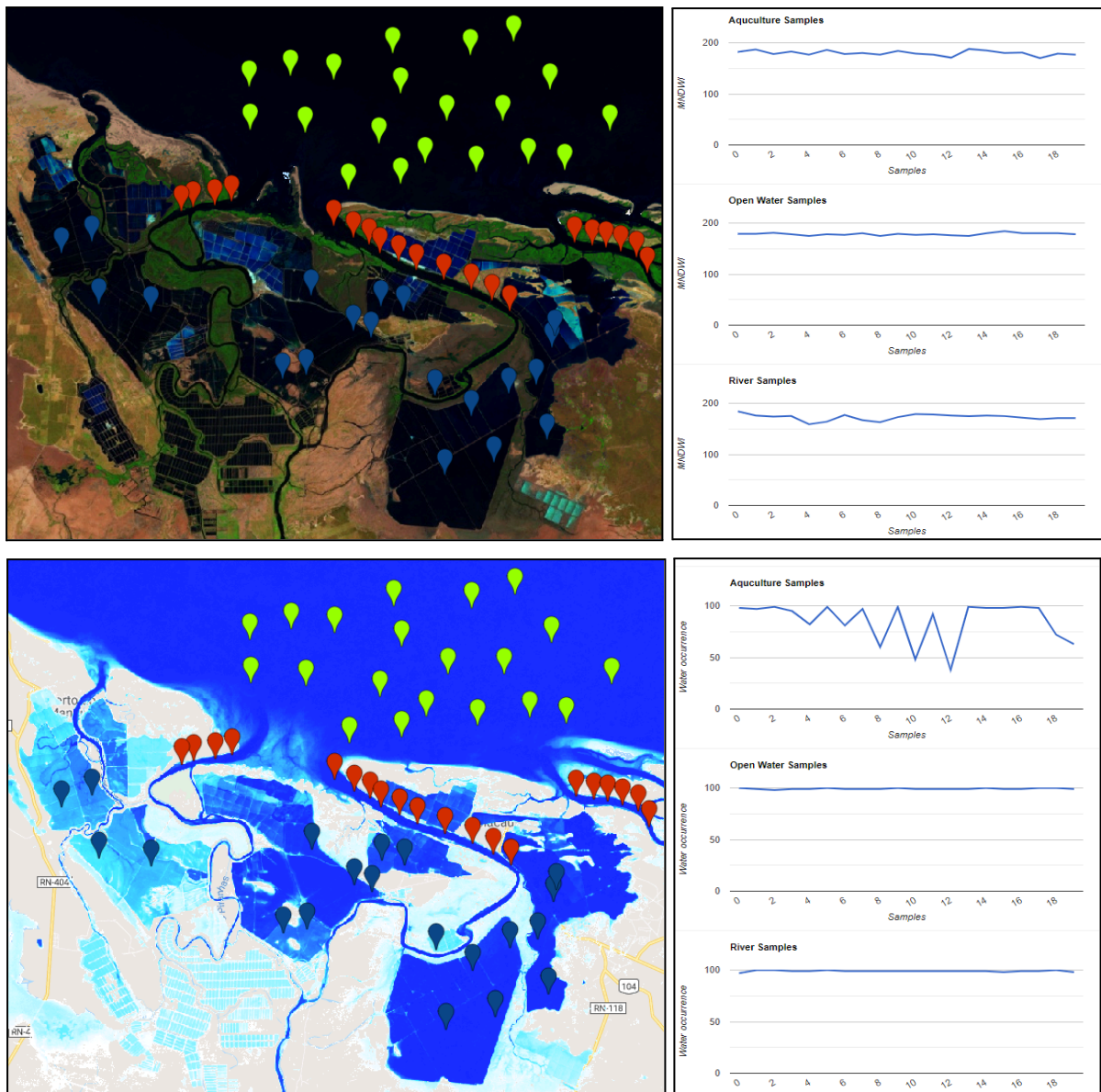


Figure 8 – Spectral and temporal patterns of the aquaculture, rivers, and open waters classes. In the top-left corner is the median cloud-free composite from Macau-RN, northeast of Brazil. The dark blue, green, and red markers represent aquaculture, open water, and river samples. On the top right are the NMDWI values for each one of the samples, in the bottom-left JRC occurrence data. The occurrence frequency of each one of the samples is at the bottom right.

In cases like this, the “context domain” may be essential to distinguishing between rivers, aquaculture, and open waters pixels. In the context analysis scenario, the U-Net: Convolutional Networks (Abadi et al., 2015) have the advantage of predicting the class label of each pixel by providing as input a local region (patches or chips) around that pixel. Such a characteristic of working with “patches” or “chips” gives the U-Net the ability to access the “context domain” of the image instead of using isolated pixels. The U-Net initial training was guided by Collection 9, visual inspection and other available reference data (Table 2).

In addition to the Brazilian coastal zone, Collection 10 now includes new areas for detection. The source for such investigation relies on the document provided by Embrapa Territorial, entitled: *Mapeamento de viveiros escavados para aquicultura no Brasil por sensoriamento remoto* (São José, F. F. de et al, 2022).

3.4.5 Shallow Coastal Reef

Collection 9 was the first MapBiomass Collection to map shallow tropical reef extent and coastal reef structures visible in satellite imagery, as shown in Figure 10, and the results are presented in a separate module within the platform. This initiative is significant, as coral reefs are the most biodiversity-dense ecosystems globally and the most diverse in the sea (Adey, 2000). Yet, it is estimated that at least 25% of all marine species depend on a healthy coral reef ecosystem for shelter, food, or reproduction during at least one phase of their life (Nancy, 2010).

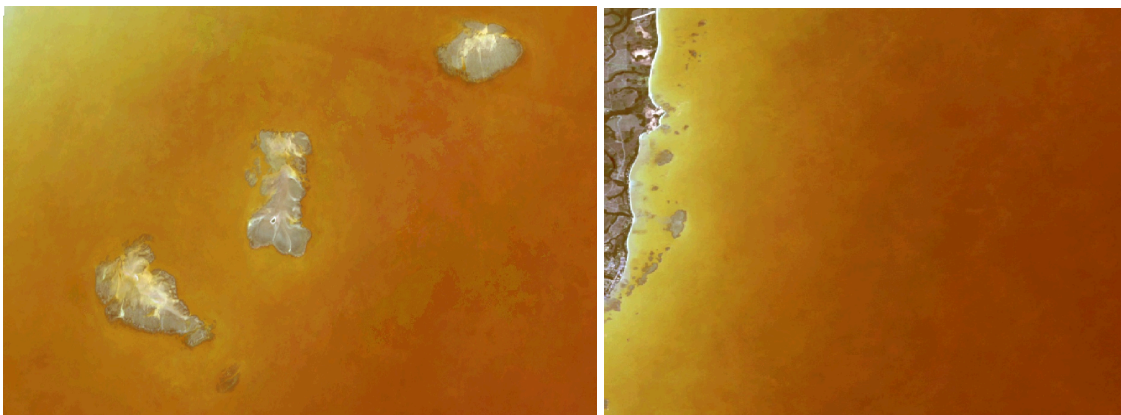


Figure 10 – Example of shallow coastal reefs - visible in satellite imagery.

This is the first approach MapBiomass has made to monitor these ecosystems. Still, the goal is to expand the mapping, indicating other essential aspects regarding the health and survival of this ecosystem. Other initiatives, such as Allen Coral Atlas (2024), have successfully mapped coral areas especially vulnerable to bleaching, inspiring us to continue studying ways to further our understanding of these ecosystems through remote sensing data. Collection 9 focuses on the shallow coral reef extent, and future collections will focus on alerting whether a given reef has crossed the environmental conditions for bleaching to occur.

The most common technical challenges regarding the automatic delineation of shallow coastal reefs are interference from suspended sediments and the depth of the reef system. In both cases, but through different mechanisms, the sun's light is prevented from reaching the reef system and scattered back by the orbital optical sensor on board satellites.

In Collection 10, additional areas were detected, following visual inspection and revisions of some deeper structures

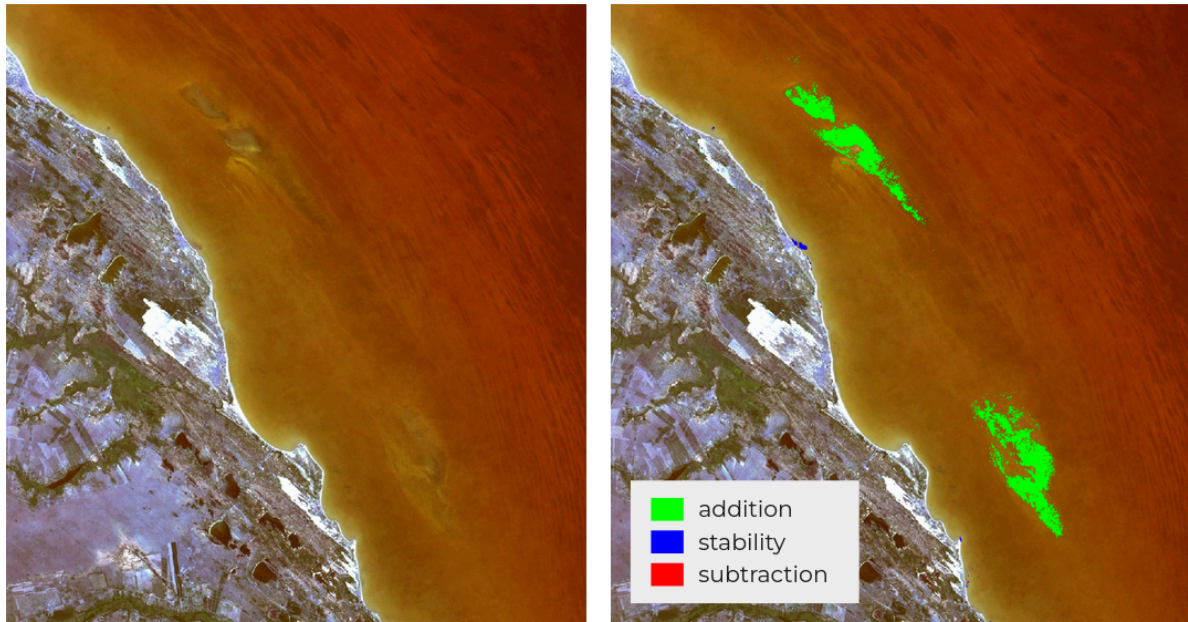


Figure 11 - Change detection between collections 9 and 10 of coastal reefs. In green, we can see some additions made to the most recent collection.

4 Post-classification

Due to the classification method's pixel-based nature and the very long temporal series, a set of post-classification filters was applied. The post-classification process includes applying a gap-fill, a temporal, a spatial, and a frequency filter.

4.1 Gap-Fill filter

The chain starts by filling in possible no-data values. In a long-time series of severely cloud-affected regions, such as tropical coastal zones, it is expected that no-data values may populate some of the resultant median composite pixels. In this filter, no-data values (“gaps”) are theoretically not allowed and are replaced by the temporally nearest valid classification. In this procedure, if no “future” valid position is available, the no-data value is replaced by its previous valid class. Up to three prior years can be used to fill in persistent no-data positions. Therefore, gaps should only exist if a given pixel has been permanently classified as no-data throughout the entire temporal domain. A mask of years was built to keep track of pixel temporal origins, as shown in Figure 12.

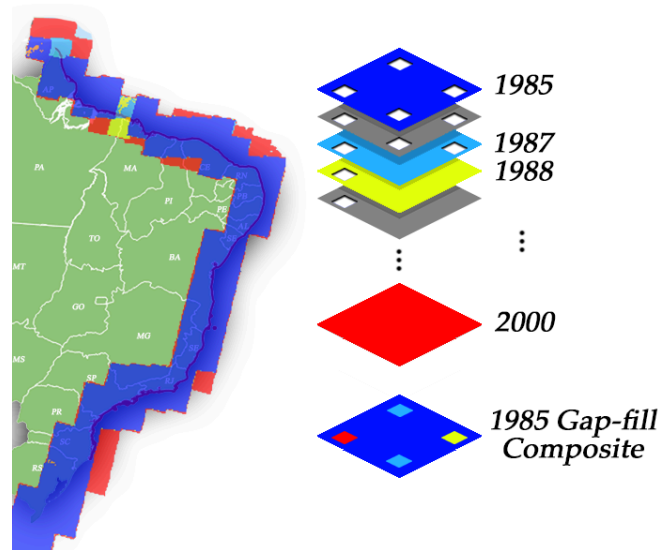


Figure 12 – Gap-filling mechanism. The following valid classification replaces existing no-data values. If no “future” valid position is available, then the no-data value is replaced by its previous valid classification based on up to a maximum of three (3) prior years. A mask of years was built to keep track of pixel temporal origins.

4.2 Temporal filter

After gap-filling, a temporal filter was executed. The temporal filter uses sequential classifications in a 3-year unidirectional moving window to identify temporally non-permitted transitions. Based on a single generic rule (GR), the temporal filter inspects the central position of three consecutive years (“ternary”). If the extremities of the ternary are identical, but the center position is not, then the central pixel is reclassified to match its temporal neighbor class, as shown in Table 6.

Table 6 - The temporal filter inspects the central position for three consecutive years, and in cases of identical extremities, the center position is reclassified to match its neighbor. T1, T2, and T3 stand for positions one (1), two (2), and three (3), respectively. GR means “generic rule”, while Mg and N-Mg represent mangrove and non-mangrove pixels.

Rule	Input (Year)			Output		
	T1	T2	T3	T1	T2	T3
GR	Mg	N-Mg	Mg	Mg	Mg	Mg
GR	N-Mg	Mg	N-Mg	N-Mg	N-Mg	N-Mg

4.3 Spatial filter

Posteriorly, a spatial filter was applied. To avoid unwanted modifications to the edges of the pixel groups (blobs), a spatial filter was built based on the "connectedPixelCount" function. Native to the GEE platform, this function locates connected components (neighbors) that share the same pixel value. Thus, only pixels that do not share connections to a predefined number of identical neighbors are considered isolated, as shown in Figure 13. This filter needs at least ten connected pixels to reach the minimum connection value.

Consequently, the minimum mapping unit is directly affected by the spatial filter applied, and it was defined as 10 pixels (~1 ha).

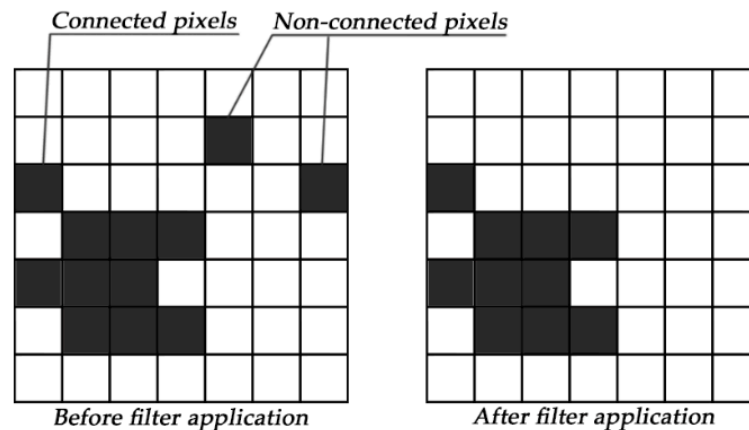


Figure 13 – The spatial filter removes pixels that do not share neighbors of identical value. The minimum connection value was 10 pixels.

4.4 Frequency filter

The last step of the filter chain is the frequency filter, as shown in Figure 14. This filter considers the occurrence frequency of a given class throughout the entire time series. Thus, all class occurrences with less than 10% temporal persistence (3 years or fewer out of 37) are filtered out and incorporated into the non-class binary. This mechanism reduces the temporal oscillation of the classification signal, decreases the number of false positives, and preserves consolidated class pixels.

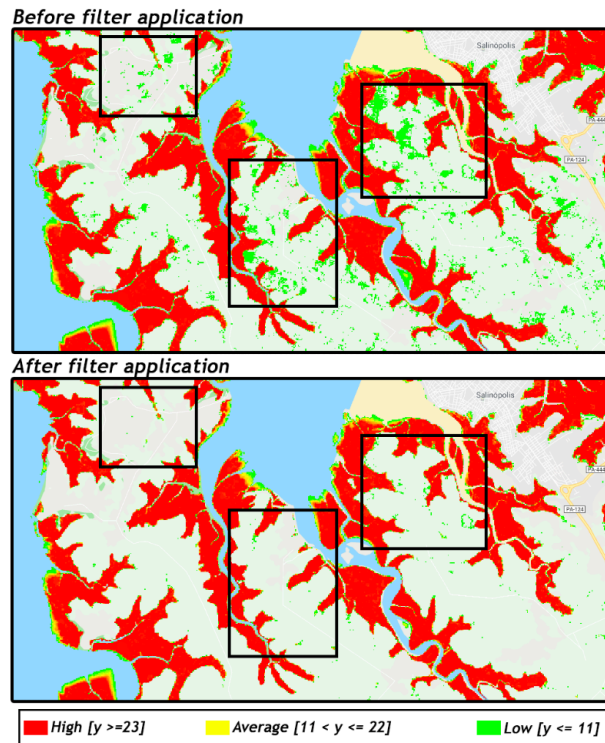


Figure 14 – Red, yellow, and green represent mangrove pixels with high (23 or more years, $y \geq 23$), average (between 11 and 22 years, $11 < y \leq 22$), and low (ten years or less, $y < 11$) occurrence frequencies, respectively. The top image shows mangrove pixels before applying the frequency filter. The bottom image shows mangrove pixels after applying the frequency filter. The black boxes are centered on areas significantly affected by the filter. All mangrove occurrences with less than 10% temporal persistence (3 years in 33 possible years) were filtered out.

4.5 Integration with biomes and cross-cutting themes

After applying the filter chain, the cross-cutting themes and the biome data are integrated. This integration is guided by specific hierarchical prevalence rules (Table 7). As the output of this step, a final land cover/land use map of Brazil for each year.

Coastal-related features such as Mangroves, Beaches, Dunes, Aquaculture, and anthropic transitions widely distributed throughout Brazil's territory tend to occupy the top positions of the prevalence rank, as seen below in Table 7.

Table 7- Prevalence rules for combining the output of digital classification with the cross-cutting themes in Collection 10.

Class	Pixel Value	Prevalence	Exception
Mining	30	1	Urban Infrastructure on MG state
Beach, Dune and Sand Spot	23	2	
Mangrove	5	3	
Aquaculture/Salt-Culture	31	4	
Hypersaline Tidal Flat	32	5	
Coastal Reefs	69	-	* coastal reefs are not integrated into the same map

References

- ABADI, M. *et al.* TensorFlow: Large-scale machine learning on heterogeneous systems. **Methods in Enzymology**, 2015.
- Adey, W. H. (2000). **Coral Reef Ecosystems and Human Health: Biodiversity Counts!** *Ecosystem Health*, 6(4), 227–236. doi:10.1046/j.1526-0992.2000.006004227.x.
- Allen Coral Atlas. Imagery, maps and monitoring of the world's tropical coral reefs, 2024. doi.org/10.5281/zenodo.3833242.
- BARBIER, E. B.; COX, M. Does Economic Development Lead to Mangrove Loss? A Cross-Country Analysis. **Contemporary Economic Policy**, v. 21, n. 4, p. 418–432, 1 out. 2003.
- BREIMAN, L. Random Forests. **Machine Learning**, v. 45, n. 1, p. 5–32, 2001.
- BUNTING, P. *et al.* **The Global Mangrove Watch—A New 2010 Global Baseline of Mangrove Extent Remote Sensing**, 2018.
- DA ROCHA, Andréa; ROTTA, Marco Aurélio; SAMPAIO, João Alfredo de; CAVALLI, Lissandra; KELLY, Cristina; BRITO, Kelly; BRITO, Benito. Overview of Fish Farming in the State of Rio Grande do Sul, Brazil. **Pesquisa Agropecuária Gaúcha**, Porto Alegre, v. 29, p. 15-37, 2024. DOI: 10.36812/pag.202430115-37.
- Diniz, C., Cortinhas, L., Nerino, G., Rodrigues, J., Sadeck, L., Adami, M., Souza-Filho, W.P., **Brazilian Mangrove Status: Three Decades of Satellite Data Analysis**. *Remote Sensing* 11, <http://dx.doi.org/10.3390/rs11070808>. 2019.
- Diniz, C., Cortinhas, L., Pinheiro, M.L., Sadeck, L., Fernandes Filho, A., Baumann, L.R.F., Adami, M., Souza-Filho, P.W.M., 2021. **A Large-Scale Deep-Learning Approach for Multi-Temporal Aqua and Salt-Culture Mapping Remote Sensing**, *Remote Sensing*, <http://dx.doi.org/10.3390/rs13081415>, 2021.
- DOMINGUEZ, J. M. L. The Coastal Zone of Brazil. *In: Geology and Geomorphology of Holocene Coastal Barriers of Brazil*. Berlin, Heidelberg: Springer Berlin Heidelberg, 2009. p. 17–51.
- ESCADAFAL, R., BELGHIT, A. AND BEN-MOUSSA, A. (1994) **Indices spectraux pour la télédétection de la dégradation des milieux naturels en Tunisie aride**. In: Guyot, G. réd., *Actes du 6eme Symposium international sur les mesures physiques et signatures en télédétection*, Val d'Isère (France), 17-24 Janvier 1994, 253-259.
- FERREIRA, B.P.; MAIDA, M.. Monitoramento dos recifes de coral do Brasil. Brasília: MMA, 2006.
- FU-MIN WANG, JING-FENG HUANG, YAN-LIN TANG, XIU-ZHEN WANG, **New Vegetation Index and Its Application in Estimating Leaf Area Index of Rice**, *Rice Science*, Volume 14, Issue 3, 2007, Pages 195-203, ISSN 1672-6308.
- GIRI, C. *et al.* Status and distribution of mangrove forests of the world using earth observation satellite data. **Global Ecology and Biogeography**, v. 20, n. 1, p. 154–159, 2011.

GITELSON, A. A., A. VIÑA, T. J. ARKEBAUER, D. C. RUNDQUIST, G. KEYDAN, AND B. LEAVITT (2003), **Remote estimation of leaf area index and green leaf biomass in maize canopies**, *Geophys. Res. Lett.*, 30, 1248, doi:10.1029/2002GL016450, 5.

GUIMARÃES, A. S. *et al.* Impact of aquaculture on mangrove areas in the northern Pernambuco Coast (Brazil) using remote sensing and geographic information system. **Aquaculture Research**, v. 41, n. 6, p. 828–838, 13 maio 2010.

ICMBIO. **Atlas dos manguezais do Brasil**. 1. ed. Brasília, Brazil: ICMBio, 2018.

KNOWLTON, Nancy, et al. Coral reef biodiversity. **Life in the world's oceans: diversity distribution and abundance**, 2010: 65-74.

LIU, H. Q.; HUETE, A. Feedback based modification of the NDVI to minimize canopy background and atmospheric noise. **IEEE Transactions on Geoscience and Remote Sensing**, 1995.

MMA. Gerência de Biodiversidade Aquática e Recursos Pesqueiros. **Panorama da conservação dos ecossistemas costeiros e marinhos no Brasil**. Brasília: MMA/SBF/GBA, 2010. 148 p.

MMA, MAPA DAS ÁREAS PRIORITÁRIAS DA ZONA COSTEIRA E MARINHA PARA CONSERVAÇÃO DA BIODIVERSIDADE. 2018. Disponível em: https://www.gov.br/mma/pt-br/assuntos/biodiversidade-e-biomas/ecossistemas/conservacao-1/areas-prioritarias/zona_costeira.jpg.

PRATES, A. P. L.; GONÇALVES, M. A.; ROSA, M. R. Panorama da conservação dos ecossistemas costeiros e marinhos no Brasil. **Brasília: MMA/SBF/GBA**, 2010.

QUEIROZ, L. *et al.* **Shrimp aquaculture in the federal state of Ceará, 1970–2012: Trends after mangrove forest privatization in Brazil**. [s.l: s.n.]. v. 73ao Óleo -Pará-Maranhão-Barreirinhas 2017.

ROGERS, A. S.; KEARNEY, M. S. Reducing signature variability in unmixing coastal marsh Thematic Mapper scenes using spectral indices. **International Journal of Remote Sensing**, 2004.

SÃO JOSÉ, F. F. DE et al. Mapeamento de viveiros escavados para aquicultura no Brasil por sensoriamento remoto. Embrapa Territorial. Documentos, 144, 2022.

SÃO JOSÉ, F. F. DE et al. Mapeamento de viveiros escavados para aquicultura no Brasil por sensoriamento remoto. Embrapa Territorial. Documentos, 144, 2022.

SOS MATA ATLÂNTICA. Atlas dos remanescentes florestais da Mata Atlântica, período 2019-2020. **São Paulo, Brasil. Fundação SOS Mata Atlântica. Instituto Nacional das Pesquisas Espaciais**, 2020.

SOSMA; INPE. ATLAS DOS REMANESCENTES FLORESTAIS DA MATA ATLÂNTICA PERÍODO 2016-2017. **Fundação SOS Mata Atlântica e Instituto de Pesquisas Espaciais**, 2018.

Souza-Filho, P.W.M., Diniz, C.G., Souza-Neto, P.W.M., Lopes, J.P.N., Nascimento Júnior, W.R., Cortinhas, L., Asp, N.E., Fernandes, M.E.B., Dominguez, J.M.L., 2023. Mangrove Swamps of Brazil: Current Status and Impact of Sea-Level Changes, in: Dominguez, J.M.L., Kikuchi, R.K.P.d., Filho, M.C.d.A., Schwamborn, R., Vital, H. (Eds.), *Tropical Marine Environments of Brazil: Spatio-Temporal Heterogeneities and Responses to Climate Changes*. Springer International Publishing, Cham, pp. 45-74, 10.1007/978-3-031-21329-8_3.

TENÓRIO, G. S. *et al.* Mangrove shrimp farm mapping and productivity on the Brazilian Amazon coast: Environmental and economic reasons for coastal conservation. **Ocean & Coastal Management**, v. 104, p. 65–77, 2015.

THOMAS, N. *et al.* Distribution and drivers of global mangrove forest change, 1996–2010. **PLOS ONE**, v. 12, n. 6, p. e0179302, 8 jun. 2017.

____. **Mapping Mangrove Extent and Change: A Globally Applicable Approach** *Remote Sensing*, 2018.

TUCKER, C. J. Red and photographic infrared linear combinations for monitoring vegetation. **Remote Sensing of Environment**, v. 8, n. 2, p. 127–150, 1979.

USGS. **LANDSAT COLLECTION 1 LEVEL 1 PRODUCT DEFINITION**. [s.l.] Earth Resources Observation and Science (EROS) Center, 2017.

XU, H. Modification of normalised difference water index (NDWI) to enhance open water features in remotely sensed imagery. **International Journal of Remote Sensing**, v. 27, n. 14, p. 3025–3033, 20 jul. 2006.